Vibration Analysis of Different Types of Porous FG Circular Sandwich Plates

Mohsen Rahmani
Faculty of Industrial and Mechanical Engineering,
Qazvin Branch, Islamic Azad University, Qazvin, Iran
E-mail: mohsen_rahmani@ymail.com

Younes Mohammadi*
Faculty of Industrial and Mechanical Engineering,
Qazvin Branch, Islamic Azad University, Qazvin, Iran
E-mail: u.mohammadi@gmail.com
*Corresponding author

Farshad Kakavand
Department of Mechanical Engineering,
Takestan Branch, Islamic Azad University, Takestan, Iran
E-mail: F.Kakavand@gmail.com

Received: 25 March 2019, Revised: 2 June 2019, Accepted: 4 August 2019

Abstract: For the first time, by applying a modified high order sandwich plates theory, vibration behaviour of two types of porous FG circular sandwich plates are investigated. In the first type, the face sheets and in the second one, the core is made of FGM which is modelled by power law rule that is modified by considering two types of porosity distributions. All materials are temperature dependent and uniform temperature distribution is used to model the effect of the temperature changing in the sandwiches. Governing equations are obtained by the Hamilton's energy principle and solved by Galerkin method for a clamped boundary condition. To verify the results, they are compared with FEM results obtained by Abaqus software and for special cases with the results in literatures.

Keywords: FG Core, FG Face-Sheets, Porosity, Temperature Dependent, Vibration

Reference: Rahmani, M., Mohammadi, Y., and Kakavand, F., "Vibration Analysis of Different Types of Porous FG Circular Sandwich Plates", Int J of Advanced Design and Manufacturing Technology, Vol. 12/No. 3, 2019, pp. 63–75.

Biographical notes: Mohsen Rahmani is a PhD candidate in Mechanical engineering in IAU, Qazvin Branch. His current research interest includes vibration, FGM, smart materials and composites. **Younes Mohammadi** is Associate Professor of Mechanical engineering at the IAU, Qazvin Branch. He received his PhD in Mechanical engineering from KNT University of Iran. His current research focuses on vibration, FGM, smart materials and composites. **Farshad Kakavand** is Associate Professor of Mechanical engineering at the IAU, Takestan Branch. He received his PhD in Mechanical engineering from Sharif University of Iran. His current research focuses on vibration and control.

1 INTRODUCTION

Nowadays, applications of sandwich structures have been increased in different modern industries. A footprint of usage of the sandwich structures has been seen in the engine aircraft, naval, space shuttle, satellite, trains, and many other engineering structures. The basic framework of sandwiches composes two, not definitely identical, face sheets which cover the core. These structures have high performance and bending rigidity versus low weight [1]. The ordinary composites are weak in high temperature environments and will fail due to delamination and stress concentration in the layers of the sandwich. So, Japanese researchers proposed functionally graded materials to overcome these problems. FGMs are microscopic inhomogeneous materials which gradually graded from a metal surface to a ceramic one [2].

These modern materials have been used in both faces and core. The material properties vary in high temperature, so the FGM and homogeneous materials which are used in the sandwiches should be considered as temperature dependent materials. Also, during the production process of FGMs, some micro voids appear which affect the material properties. Different porosity distributions are considered to model the micro voids such as even and uneven porosity [3]. Shear deformation plate theory, 3D elastic theory, energy and finite element method are some approaches to investigate the mechanical behaviour of sandwich panels [4]. In these theories, the core height is constant, but in fact the thickness of the sandwich plates are variable. So, the core should be considered as a flexible layer that is compressed transversely. In the classical theories, the localized effects in the core cannot be calculated, so to consider these effects the high order theory was presented [5]. An important kind of sandwich structures that is used in high temperature industries is the FG circular sandwich plate with both FG faces and FG core. FGMs have wide applications in the researches. Najafzadeh and Shoughi studied the vibration behaviour of functionally graded circular plate with various boundary conditions [6]. Zenkour and sobhy investigated the buckling of the sandwich plates and applied the FGMs as the faces which their material properties varied gradually by a power law rule along the thickness [7]. Amininejad et al. investigated the vibration of FG plates with classical boundary conditions. The FGM properties were graded based on a sigmoid function [8]. Davar et al. studied the vibration behaviour of FG circular cylindrical shells under internal pressure. The material properties varied based on a power law rule [9]. Kamarian presented a volume fraction optimization for FGM beams resting on elastic foundation. The properties graded through the thickness based on a generalized power-law rule [10]. Boutahar and Benamar investigated the vibration behaviour of porous FG annular plates with elastic foundations. They modified the mixture rule by considering the porosity of FGM [3].

Wang and Zu surveyed the vibration of the porous FG rectangular plates in different thermal conditions. Defects in production process result in considering two types of porosity distribution, namely, even and uneven [11]. Barati and Shahverdi analysed the stability of supersonic porous FGM panels by using a high order theory. They used even and uneven distributions to model the porosities [12]. Chen et al. studied some mechanical behaviour of FG porous beam by applying the Timoshenko theory. They considered the material properties of the composite varied along the thickness by various porosity distributions [13]. By applying a finite element approach, Prakash and Ganapathi studied the mechanical behaviour of FG circular plates [14]. Heydari by using energy method studied the buckling of FG circular plates [15].

Jandaghian and Jafari by using Kirchhoff plate model studied the vibration of a circular plate [16]. Morovat by applying the high order sandwich shell theory studied the buckling of composite sandwich truncated conical shells [17]. Mantari et al. utilised a HSDT to find the frequencies of functionally graded plates located on elastic foundation [18]. Khalili and Mohammadi by applying a high order theory of the sandwich plates investigated the vibration behaviours of a FG rectangular sandwich plates [19]. With a high order theory Salami et al. inspected the bending in rather thick faces sandwich beams with a soft core which satisfied the stress compatibility condition at interface [20]. Frostig et al. investigated the nonlinear wrinkling of a functionally graded core sandwich panel by employing a modified high order theory [21]. Temperature dependent materials have been used in some researches. Shahrjerdi et al. analyzed the vibration characteristics of temperature-dependent solar FG plates by applying the second-order shear deformation theory [22].

Frostig and Thomsen numerically investigated the vibration of sandwich plates consisted of a core that its material was temperature dependent [23]. Pandey and Pradyumna by utilising the layer-wise theory, explored the frequency responses of the FG sandwich plates made of the temperature dependent materials [24]. Many researchers have explored the vibration behaviour of the circular sandwich plates. Sherif discussed the frequencies characteristics of the clamped circular sandwich plates by applying the FSDT. The core was viscoelastic and shear stress and rotary inertia were considered [25]. Chan II Park derived the frequency equations of the uniform thickness circular plate with clamped boundary condition [26]. By exerting a 3D elasticity procedure, Nie and Zhong investigated the frequencies characteristic of the FG circular plates in various boundary conditions [27]. Ebrahimi et al. studied the vibration characteristics of FG circular plate which was merged with two piezoelectric layers in different boundary condition [28]. Lal and Rani investigated the free vibrations of circular sandwich plates in different boundary conditions by utilising the FSDT [29]. Heshmati and Jalali studied the vibration of porous FG circular and annular sandwich plates based on the FSDT [30].

As a result of review in the accessible literatures, it is found that more investigation into the free vibration of circular sandwich plates is needed. This study thus intends to scrutinize the temperature dependent vibration behaviour of sandwich circular plates with FG faces and FG core based on the high order sandwich plate theory. The differences of this study in comparison with the other researches are as follows:

1- Applying the high order sandwich plate theory which is modified by considering the flexibility of the core in the thickness direction.

2- Considering the high order stresses and thermal stress resultants, in plane stresses and thermal stresses of the core and face sheets at the same time.

3- Considering porosity distributions in both FG faces and FG core.

4- Considering the dependency of temperature for all materials properties of sandwiches.

Two kinds of circular sandwich plates are considered in the uniform temperature distributions. In the first type, sandwiches consist of two FG faces which cover a homogeneous core, namely, type-I and in the second type, sandwiches with FG core which surrounded by two homogeneous face sheets, namely, type-II. FGM properties are temperature and location dependent which are graded according to power law rules that include the volume fraction of the porosities.

Boundary condition is clamped and equations are derived based on the Hamilton's energy principle. To obtain the frequencies, a Galerkin method is applied. In order to validate the present approach, the results of this analytical approach are compared with the numerical results which were obtained by Abaqus software and for a special case are compared with some literatures. Finally, the effects of the temperature changing, volume fraction distribution of FG face sheets and FG core, porosity and some geometrical effects on the vibration characteristics of defined sandwich plates are investigated.

2 BASIC FORMULATION

In this study, FGMs are used in the face sheets and the core in two types of sandwich. First, a sandwich with FG face sheets and a homogeneous core, named, type-I and second, a sandwich with a FG core and two homogeneous face sheets. In order to investigate the vibration behaviour of functionally graded circular sandwich plates and obtain the governing equations of the motion, Hamilton's energy principle is applied which consists of the variation of the kinetic, δK, and strain energy, δU. The main equation is as follow [31]:

$$\int_{t1}^{t2}\left(-\delta K+\delta U\right)dt=0 \tag{1}$$

The variation of the kinetic energy is calculated as follows:

$$\begin{aligned}\int_{t1}^{t2}\delta K dt=&\int_{t1}^{t2}\{\int_0^a\int_0^{2\pi}\int_{-\frac{h_t}{2}}^{\frac{h_t}{2}}\rho_t(\ddot{u}_t\delta u_t+\ddot{\upsilon}_t\delta\upsilon_t+\ddot{w}_t\delta w_t)rdrd\theta dz_t+\\&\int_0^a\int_0^{2\pi}\int_{-\frac{h_b}{2}}^{\frac{h_b}{2}}\rho_b(\ddot{u}_b\delta u_b+\ddot{\upsilon}_b\delta\upsilon_b+\ddot{w}_b\delta w_b)rdrd\theta dz_b\\&+\int_0^a\int_0^{2\pi}\int_{-\frac{h_c}{2}}^{\frac{h_c}{2}}\rho_c(\ddot{u}_c\delta u_c+\ddot{\upsilon}_c\delta\upsilon_c+\ddot{w}_c\delta w_c)rdrd\theta dz_c\}dt\end{aligned} \tag{2}$$

where $(\ddot{\cdot})$ indicates the second derivative with respect to time; the density is "ρ" which in the functionally graded layers is the function of the displacement and the temperature, and in the homogeneous layer is just a function of the temperature; the top and bottom face sheets and the core, are indicated with "t", "b" and "c", respectively. To model the properties of the FGMs which usually include ceramic and metal and vary gradually in the thickness direction, a power law rule is applied. By considering two kinds of porosity distribution which appear in the manufacturing process, the power law rule is modified to approach an accurate prediction of the material properties. The first one is even porosity distribution that modifies the power law rule as follows [3]:

$$\begin{aligned}P_j\left(z_j,T\right)=&g\left(z_j\right)P_{ce}^j\left(T\right)+\left[1-g\left(z_j\right)\right]P_m^j\left(T\right)-\\&(P_{ce}^j\left(T\right)+P_m^j\left(T\right))\frac{\zeta}{2},\quad j=(t,b,c)\end{aligned} \tag{3}$$

$$g\left(z_o\right)=\left(\frac{\frac{h_o}{2}-z_o}{h_o}\right)^N;\ g\left(z_i\right)=\left(\frac{\frac{h_i}{2}+z_i}{h_i}\right)^N;\quad g\left(z_c\right)=\left(\frac{\frac{h_c}{2}-z_c}{h_c}\right)^N \tag{4}$$

Where "ζ" is the porosity volume fraction. It is assumed that the porosities occurred at the middle area when the FGM structures have been produced based on the principle of multi-step sequential infiltration techniques. In this area, infiltration of the material is hard and imperfect but at the edges of the FG layer, it has been performed easily that causes to less porosity. So, in the second approximation, it is considered that the porosities are distributed in the middle area of the FG layer and by approaching to the edges, they decrease and tend to the zero. Therefore, the equation of the material properties in the uneven case are modified as follows [3]:

$$P_j\left(z_j,T\right)=g\left(z_j\right)P_{ce}^j\left(T\right)+\left[1-g\left(z_j\right)\right]P_m^j\left(T\right)-\left(P_{ce}^j\left(T\right)+P_m^j\left(T\right)\right)\frac{\zeta}{2}\left(1-\frac{2|z|}{h}\right) \tag{5}$$

Since these sandwich structures are applied in high temperature conditions, it is necessary to consider that the FGMs and homogeneous materials are temperature dependent. This dependency is expressed as a nonlinear function of temperature as follows [32]:

$$P=C_0\left(C_{-1}T^{-1}+1+C_1T+C_2T^2+C_3T^3\right) \tag{6}$$

Where "C"s are unique coefficients of temperature for each material, and $T=T_0+\Delta T$, which T_0 is the room temperature. Inspired by Kirchhoff's assumptions, a classical theory of plates in polar coordinate, is employed to model the displacement fields of the face-sheets as [33]:

$$u_j\left(r,\theta,z,t\right)=u_{0j}\left(r,\theta,t\right)-z_j\frac{\partial w\left(r,\theta,t\right)}{\partial r} \tag{7}$$

$$\upsilon_j\left(r,\theta,z,t\right)=\upsilon_{0j}\left(r,\theta,t\right)-\frac{z_j}{r}\frac{\partial w\left(r,\theta,t\right)}{\partial r},\ (j=t,b) \tag{8}$$

$$w_j\left(r,\theta,z,t\right)=w_{0j}\left(r,\theta,t\right) \tag{9}$$

Where "0" denotes values with correspondence to the central plane of the layers. "u" and "υ" are the in-plane deformations in the "r" and "θ" directions and "w" is the transverse deflections of the faces as shown in "Fig. 1". Figure 1 shows a schematic of functionally graded circular sandwich plate which faces are FGM in type-I and core is FGM in type-II.

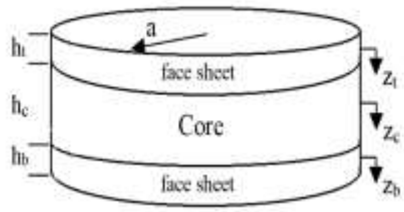

Fig. 1 A schematic of circular FG sandwich plate.

Also, the kinematic relations of the core are considered as the polynomial pattern with the unknown coefficients, u_k and v_k (k= 0,1,2,3), for the in-plane and w_l (l = 0,1,2) for vertical displacement components which are obtained by the variational principle [19]:

$$u_c\left(r,\theta,z_c,t\right)=u_0\left(r,\theta,t\right)+u_1\left(r,\theta,t\right)z_c+u_2\left(r,\theta,t\right)z_c^2+u_3\left(r,\theta,t\right)z_c^3 \tag{10}$$

$$v_c\left(r,\theta,z_c,t\right)=v_0\left(r,\theta,t\right)+v_1\left(r,\theta,t\right)z_c+v_2\left(r,\theta,t\right)z_c^2+v_3\left(r,\theta,t\right)z_c^3 \tag{11}$$

$$w_c\left(r,\theta,z_c,t\right)=w_0\left(r,\theta,t\right)+w_1\left(r,\theta,t\right)z_c+w_2\left(r,\theta,t\right)z_c^2 \tag{12}$$

In this theory, the compatibility conditions assume that the faces are sticked to the core completely and the interface displacements between the core and the face sheets can be obtained as follows:

$$\begin{aligned}&u_c\left(z_c=-h_c/2\right)=u_t\left(z_t=h_t/2\right);\\&\upsilon_c\left(z_c=-h_c/2\right)=\upsilon_t\left(z_t=h_t/2\right);\\&w_c\left(z_c=-h_c/2\right)=w_t\end{aligned} \tag{13}$$

$$\begin{aligned}&u_b\left(z_b=-h_b/2\right)=u_c\left(z_c=h_c/2\right);\\&\upsilon_b\left(z_b=-h_b/2\right)=\upsilon_c\left(z_c=h_c/2\right);\\&w_b=w_c\left(z_c=h_c/2\right)\end{aligned} \tag{14}$$

The variation of the total strain energy includes all mechanical and thermal stresses and linear and nonlinear strains of the layers of the sandwich plates that make the mechanical and thermal energy [34]. In addition, the compatibility conditions at the interfaces of the core and the face-sheets are the constraints and attended in the Hamilton's principle in terms of six Lagrange multipliers. By considering the effects in-plane stresses of the core in this formulation, δU, is as follows:

$$\delta U = \int_{V_t} (\sigma_{rr}^{t}\delta\varepsilon_{rr}^{t} + \sigma_{rr}^{tT}\delta d_{rr}^{t} + \sigma_{\theta\theta}^{t}\delta\varepsilon_{\theta\theta}^{t} + \sigma_{\theta\theta}^{tT}\delta d_{\theta\theta}^{t} + \tau_{r\theta}^{t}\delta\gamma_{r\theta}^{t})dV$$
$$+\int_{V_b} (\sigma_{rr}^{b}\delta\varepsilon_{rr}^{b} + \sigma_{rr}^{bT}\delta d_{rr}^{b} + \sigma_{\theta\theta}^{b}\delta\varepsilon_{\theta\theta}^{b} + \sigma_{\theta\theta}^{bT}\delta d_{\theta\theta}^{b} + \tau_{r\theta}^{b}\delta\gamma_{r\theta}^{b})dV$$
$$+\int_{V_{core}} (\sigma_{rr}^{c}\delta\varepsilon_{rr}^{c} + \sigma_{\theta\theta}^{c}\delta\varepsilon_{\theta\theta}^{c} + \sigma_{zz}^{c}\delta\varepsilon_{zz}^{c} + \tau_{r\theta}^{c}\delta\gamma_{r\theta}^{c} + \tau_{rz}^{c}\delta\gamma_{rz}^{c} + \tau_{\theta z}^{c}\delta\gamma_{\theta z}^{c})dV$$
$$+\delta\int_0^a\int_0^{2\pi}[\lambda_{rt}\left(u_t\left(z_t = h_t/2\right) - u_c\left(z_c = -h_c/2\right)\right)$$
$$+\lambda_{\theta t}\left(\upsilon_t\left(z_t = h_t/2\right) - \upsilon_c\left(z_c = -h_c/2\right)\right) + \tag{15}$$
$$\lambda_{zt}\left(w_t - w_c\left(z_c = -h_c/2\right)\right) +$$
$$\lambda_{rb}\left(u_c\left(z_c = h_c/2\right) - u_b\left(z_b = -h_b/2\right)\right) +$$
$$\lambda_{\theta b}\left(\upsilon_c\left(z_c = h_c/2\right) - \upsilon_b\left(z_b = -h_b/2\right)\right) +$$
$$\lambda_{zb}\left(w_c\left(z_c = h_c/2\right) - w_b\right)]rdrd\theta$$

"σ_{rr}", "$\sigma_{\theta\theta}$" and "$\tau_{r\theta}$" display the normal and shear stresses, "ε_{rr}", "$\varepsilon_{\theta\theta}$" and "$\gamma_{r\theta}$" are the linear normal and shear strains of the layers, "σ_{rr}^{T}" and "$\sigma_{\theta\theta}^{T}$" express the thermal stresses and "d_{rr}" and "$d_{\theta\theta}$" are the non-linear strains in the faces, "σ_{zz}^{c}" and "ε_{zz}^{c}" present the lateral normal stress and strain in the core, "τ_{rz}^{c}", "$\tau_{\theta z}^{c}$", "γ_{rz}^{c}"and "$\gamma_{\theta z}^{c}$" declare the shear stresses and shear strains in the thickness direction of the core, "λ_r","λ_θ" and "λ_z" are the Lagrange multipliers at the face sheet-core interfaces. Considering small deflection, the strain components for the faces can be declared as follows [34]:

$$\varepsilon_{rr}^{j}\left(r,\theta,z_j,t\right) = u_{0j,r}\left(r,\theta,t\right) - z_j w_{j,rr}\left(r,\theta,t\right) + \frac{1}{2}\left(w_{j,r}\right)^2 \tag{16}$$

$$\varepsilon_{\theta\theta}^{j}\left(r,\theta,z_j,t\right) = \frac{1}{r^2}\{ru_{0j}\left(r,\theta,t\right) - r\upsilon_{0j,\theta}\left(r,\theta,t\right) - z_j w_{j,\theta\theta}\left(r,\theta,t\right) - rz_j w_{j,r}\left(r,\theta,t\right)\} + \frac{1}{2}\left(\frac{w_{j,\theta}}{r}\right)^2 \tag{17}$$

$$\varepsilon_{r\theta}^{j}\left(r,\theta,z_j,t\right) = \frac{1}{r^2}\{ru_{0j,\theta}\left(r,\theta,t\right) + r^2\upsilon_{0j,r}\left(r,\theta,t\right) - r\upsilon_{0j}\left(r,\theta,t\right) + 2z_j w_{j,\theta}\left(r,\theta,t\right) - 2rz_j w_{j,r\theta}\left(r,\theta,t\right)\} \tag{18}$$

The"$()_{,i}$" expresses derivation with respect to i. The strain of the core can be defined as [35]:

$$\varepsilon_{rr}^{c} = u_{0,r}^{\ c} + z_c u_{1,r}^{\ c} + z_c^{\ 2} u_{2,r}^{\ c} + z_c^{\ 3} u_{3,r}^{\ c} \tag{19}$$

$$\varepsilon_{\theta\theta}^{c} = \frac{1}{r}[\upsilon_{0,\theta}^{\ c} + z_c\upsilon_{1,\theta}^{\ c} + z_c^{\ 2}\upsilon_{2,\theta}^{\ c} + z_c^{\ 3}\upsilon_{3,\theta}^{\ c}] + \frac{1}{r}[u_0^{\ c} + z_c u_1^{\ c} + z_c^{\ 2}u_2^{\ c} + z_c^{\ 3}u_3^{\ c}] \tag{20}$$

$$\varepsilon_{r\theta}^{c} = \frac{1}{r}\left[u_{0,\theta}^{\ c} + z_c u_{1,\theta}^{\ c} + z_c^{\ 2}u_{2,\theta}^{\ c} + z_c^{\ 3}u_{3,\theta}^{\ c}\right] + \left[\upsilon_{0,\theta}^{\ c} + z_c\upsilon_{1,\theta}^{\ c} + z_c^{\ 2}\upsilon_{2,\theta}^{\ c} + z_c^{\ 3}\upsilon_{3,\theta}^{\ c}\right] - \frac{1}{r}\left[\upsilon_0^{\ c} + z_c\upsilon_1^{\ c} + z_c^{\ 2}\upsilon_2^{\ c} + z_c^{\ 3}\upsilon_3^{\ c}\right] \tag{21}$$

$$\varepsilon_{rz}^{c} = \left[u_1^{\ c} + 2u_2^{\ c}z_c + 3u_3^{\ c}z_c^{\ 2}\right] + \left[w_{0,r}^{\ c} + z_c w_{1,r}^{\ c} + z_c^{\ 2}w_{2,r}^{\ c}\right] \tag{22}$$

$$\varepsilon_{\theta z}^{c} = \left[\upsilon_1^{\ c} + 2\upsilon_2^{\ c}z_c + 3\upsilon_3^{\ c}z_c^{\ 2}\right] + \frac{1}{r}\left[w_{0,r}^{\ c} + z_c w_{1,r}^{\ c} + z_c^{\ 2}w_{2,r}^{\ c}\right] \tag{23}$$

$$\varepsilon_{zz}^{c} = \left[w_1^{\ c} + 2w_2^{\ c}z_c\right] \tag{24}$$

In this model, by substituting the expressions of the "Eq. (2) and Eq. (15)" according to the kinematic relations of the layers and using the interfaces relations, and after some algebraic operations, the twenty-three equations of motion are obtained, which included twenty-three unknowns: six displacement unknowns for both face sheets in "Eqs. (25-30)", eleven displacement unknowns for the core in "Eqs. (31-41)", and six Lagrange multipliers in "Eqs. (42-47)":

$$-I_{0t}\ddot{u}_{0t}r+I_{1t}r\ddot{w}_{t,r}-N^{t}_{rr}-rN^{t}_{rr,r}+N^{t}_{\theta\theta}-N^{t}_{r\theta,\theta}+r\lambda_{rt}=0 \tag{25}$$

$$-I_{0t}\ddot{v}_{0t}r+I_{1t}\ddot{w}_{t,\theta}-N^{t}_{\theta\theta,\theta}-rN^{t}_{r\theta,r}-2N^{t}_{r\theta}+r\lambda_{\theta t}=0 \tag{26}$$

$$\begin{aligned}&-I_{1t}\ddot{u}_{0t}-I_{1t}r\ddot{u}_{0t,r}+I_{2t}\ddot{w}_{t,r}+I_{2t}r\ddot{w}_{t,rr}-I_{1t}\ddot{v}_{0t,\theta}+\frac{I_{2t}}{r}\ddot{w}_{t,\theta\theta}-I_{0t}r\ddot{w}_{t}\\&-2M^{t}_{rr,r}-rM^{t}_{rr,rr}-\frac{1}{r}M^{t}_{\theta\theta,\theta\theta}+M^{t}_{\theta\theta,r}-\frac{2}{r}M^{t}_{r\theta,\theta}-2M^{t}_{r\theta,r\theta}-\\&N^{tT}_{rr}w_{t,r}-rN^{tT}_{rr,r}w_{t,r}-rN^{tT}_{rr}w_{t,rr}-\frac{N^{tT}_{\theta\theta,\theta}}{r}w_{t,\theta}-\frac{N^{tT}_{\theta\theta}}{r}w_{t,\theta\theta}+\\&\frac{h_t}{2}\lambda_{rt}+\frac{rh_t}{2}\frac{\partial\lambda_{rt}}{\partial r}+\frac{h_t}{2}\frac{\partial\lambda_{\theta t}}{\partial\theta}+r\lambda_{zt}=0\end{aligned} \tag{27}$$

$$-I_{0b}\ddot{u}_{0b}r+I_{1b}r\ddot{w}_{b,r}-N^{b}_{rr}-rN^{b}_{rr,r}+N^{b}_{\theta\theta}-N^{b}_{r\theta,\theta}-r\lambda_{\theta b}=0 \tag{28}$$

$$-I_{0b}\ddot{v}_{0b}r+I_{1b}\ddot{w}_{b,\theta}-N^{b}_{\theta\theta,\theta}-rN^{b}_{r\theta,r}-2N^{b}_{r\theta}-r\lambda_{\theta b}=0 \tag{29}$$

$$\begin{aligned}&-I_{1b}\ddot{u}_{0b}-I_{1b}r\ddot{u}_{0b,r}+I_{2b}\ddot{w}_{b,r}+I_{2b}r\ddot{w}_{b,rr}-I_{1b}\ddot{v}_{0b,\theta}+\frac{I_{2b}}{r}\ddot{w}_{b,\theta\theta}\\&-I_{0b}r\ddot{w}_{b}-2M^{b}_{rr,r}-rM^{b}_{rr,rr}-\frac{1}{r}M^{b}_{\theta\theta,\theta\theta}+M^{b}_{\theta\theta,r}-\frac{2}{r}M^{b}_{r\theta,\theta}-\\&2M^{b}_{r\theta,r\theta}-N^{bT}_{rr}w_{b,r}-rN^{bT}_{rr,r}w_{b,r}-rN^{bT}_{rr}w_{b,rr}-\frac{N^{bT}_{\theta\theta,\theta}}{r}w_{b,\theta}-\\&\frac{N^{bT}_{\theta\theta}}{r}w_{b,\theta\theta}+\frac{h_b}{2}\lambda_{rb}+\frac{rh_b}{2}\frac{\partial\lambda_{rb}}{\partial r}+\frac{h_b}{2}\frac{\partial\lambda_{\theta b}}{\partial\theta}+r\lambda_{zb}=0\end{aligned} \tag{30}$$

$$\begin{aligned}&-I_{0c}r\ddot{u}_{0c}-I_{1c}r\ddot{u}_{1c}-I_{2c}r\ddot{u}_{2c}-I_{3c}r\ddot{u}_{3c}-R^{c}_{rr}-rR^{c}_{rr,r}+R^{c}_{\theta}\\&-Q^{c}_{r\theta,\theta}-r\lambda_{rt}+r\lambda_{rb}=0\end{aligned} \tag{31}$$

$$\begin{aligned}&-I_{1c}r\ddot{u}_{0c}-I_{2c}r\ddot{u}_{1c}-I_{3c}r\ddot{u}_{2c}-I_{4c}r\ddot{u}_{3c}-M^{c}_{r1}-rM^{c}_{r1,r}\\&+M^{c}_{\theta1}+rQ_{rc}-M^{c}_{Q1r\theta,\theta}+\frac{h_c}{2}r\lambda_{rt}+\frac{h_c}{2}r\lambda_{rb}=0\end{aligned} \tag{32}$$

$$\begin{aligned}&-I_{2c}r\ddot{u}_{0c}-I_{3c}r\ddot{u}_{1c}-I_{4c}r\ddot{u}_{2c}-I_{5c}r\ddot{u}_{3c}-M^{c}_{r2}-rM^{c}_{r2,r}\\&+M^{c}_{\theta2}+2rM_{Q1rc}-M^{c}_{Q2r\theta,\theta}-\frac{h_c^{2}}{4}r\lambda_{rt}+\frac{h_c^{2}}{4}r\lambda_{rb}=0\end{aligned} \tag{33}$$

$$\begin{aligned}&-I_{3c}r\ddot{u}_{0c}-I_{4c}r\ddot{u}_{1c}-I_{5c}r\ddot{u}_{2c}-I_{6c}r\ddot{u}_{3c}-M^{c}_{r3}-rM^{c}_{r3,r}+\\&M^{c}_{\theta3}+3rM_{Q2rc}-M^{c}_{Q3r\theta,\theta}+\frac{h_c^{3}}{8}r\lambda_{rt}+\frac{h_c^{3}}{8}r\lambda_{rb}=0\end{aligned} \tag{34}$$

$$\begin{aligned}&-I_{0c}r\ddot{v}_{0c}-I_{1c}r\ddot{v}_{1c}-I_{2c}r\ddot{v}_{2c}-I_{3c}r\ddot{v}_{3c}-R^{c}_{\theta,\theta}-2Q^{c}_{r\theta}\\&+rQ^{c}_{r\theta,r}-r\lambda_{\theta t}+r\lambda_{\theta b}=0\end{aligned} \tag{35}$$

$$\begin{aligned}&-I_{1c}r\ddot{v}_{0c}-I_{2c}r\ddot{v}_{1c}-I_{3c}r\ddot{v}_{2c}-I_{4c}r\ddot{v}_{3c}-M^{c}_{\theta1,\theta}+Q_{\theta c}r-\\&2M_{Q1r\theta}-rM^{c}_{Q1r\theta,r}+\frac{h_c}{2}r\lambda_{\theta t}+\frac{h_c}{2}r\lambda_{\theta b}=0\end{aligned} \tag{36}$$

$$\begin{aligned}&-I_{2c}r\ddot{v}_{0c}-I_{3c}r\ddot{v}_{1c}-I_{4c}r\ddot{v}_{2c}-I_{5c}r\ddot{v}_{3c}-M^{c}_{\theta2,\theta}+\\&2rM_{Q1\theta c}-2M^{c}_{Q2r\theta}-rM^{c}_{Q2r\theta,r}-\frac{h_c^{2}}{4}r\lambda_{\theta t}+\\&\frac{h_c^{2}}{4}r\lambda_{\theta b}=0\end{aligned} \tag{37}$$

$$\begin{aligned}&-I_{3c}r\ddot{v}_{0c}-I_{4c}r\ddot{v}_{1c}-I_{5c}r\ddot{v}_{2c}-I_{6c}r\ddot{v}_{3c}-M^{c}_{\theta3,\theta}+\\&3rM_{Q2\theta c}-2M^{c}_{Q3r\theta}-rM^{c}_{Q3r\theta,r}+\frac{h_c^{3}}{8}r\lambda_{\theta t}+\frac{h_c^{3}}{8}r\lambda_{\theta b}=0\end{aligned} \tag{38}$$

$$\begin{aligned}&-I_{0c}r\ddot{w}_{0c}-I_{1c}r\ddot{w}_{1c}-I_{2c}r\ddot{w}_{2c}-Q^{c}_{\theta c,\theta}-Q^{c}_{rc}-rQ^{c}_{rc,r}\\&-r\lambda_{zt}-r\lambda_{zb}=0\end{aligned} \tag{39}$$

$$\begin{aligned}&-I_{1c}r\ddot{w}_{0c}-I_{2c}r\ddot{w}_{1c}-I_{3c}r\ddot{w}_{2c}+-rR^{c}_{z}-\frac{\partial M^{c}_{Q1\theta c,\theta}}{\partial\theta}-M_{Q1rc}\\&-rM^{c}_{Q1rc,r}+\frac{h_c}{2}r\lambda_{zt}-\frac{h_c}{2}r\lambda_{zb}=0\end{aligned} \tag{40}$$

$$\begin{aligned}&-I_{2c}r\ddot{w}_{0c}-I_{3c}r\ddot{w}_{1c}-I_{4c}r\ddot{w}_{2c}+2rM^{c}_{z}-M^{c}_{Q2\theta c,\theta}-M^{c}_{Q2rc}\\&-rM^{c}_{Q2rc,r}-\frac{h_c^{2}}{4}r\lambda_{zt}+\frac{h_c^{2}}{4}r\lambda_{zb}=0\end{aligned} \tag{41}$$

$$u_{0t}-\frac{h_t}{2}\frac{\partial w_t}{\partial r}-u_{0c}+\frac{h_c}{2}u_{1c}-\frac{h_c^{2}}{4}u_{2c}+\frac{h_c^{3}}{8}u_{3c}=0 \tag{42}$$

$$v_{0t}-\frac{h_t}{2r}\frac{\partial w_t}{\partial\theta}-v_{0c}+\frac{h_c}{2}v_{1c}-\frac{h_c^{2}}{4}v_{2c}+\frac{h_c^{3}}{8}v_{3c}=0 \tag{43}$$

$$\mathrm{w}_{0t}-\mathrm{w}_{0c}+\frac{\mathrm{h_c}}{2}\mathrm{w}_{1c}-\frac{\mathrm{h_c}^{2}}{4}w_{2c}=0 \tag{44}$$

$$u_{0c}+\frac{h_c}{2}u_{1c}+\frac{h_c^{\ 2}}{4}u_{2c}+\frac{h_c^{\ 3}}{8}u_{3c}-u_{0b}-\frac{h_b}{2}\frac{\partial w_b}{\partial r}=0 \quad (45)$$

$$\nu_{0c}+\frac{h_c}{2}\nu_{1c}+\frac{h_c^{\ 2}}{4}\nu_{2c}+\frac{h_c^{\ 3}}{8}\nu_{3c}-\nu_{0b}-\frac{h_b}{2r}\frac{\partial w_b}{\partial \theta}=0 \quad (46)$$

$$w_{0c}+\frac{h_c}{2}w_{1c}+\frac{h_c^{\ 2}}{4}w_{2c}-w_{0b}=0 \quad (47)$$

In the relations of the face sheets, the "N"s depict the stress resultants and the "M"s refer to the moment resultants which calculated as follows:

$$\begin{bmatrix} N_{rr}^{j} \\ N_{\theta\theta}^{j} \\ N_{r\theta}^{j} \\ M_{rr}^{j} \\ M_{\theta\theta}^{j} \\ M_{r\theta}^{j} \end{bmatrix}=\begin{bmatrix} A_{11}^j & A_{12}^j & 0 & B_{11}^j & B_{12}^j & 0 \\ A_{12}^j & A_{22}^j & 0 & B_{12}^j & B_{22}^j & 0 \\ 0 & 0 & A_{66}^j & 0 & 0 & B_{66}^j \\ B_{11}^j & B_{12}^j & 0 & D_{11}^j & D_{12}^j & 0 \\ B_{12}^j & B_{22}^j & 0 & D_{12}^j & D_{22}^j & 0 \\ 0 & 0 & B_{66}^j & 0 & 0 & D_{66}^j \end{bmatrix}\begin{bmatrix} \varepsilon_{rr}^0 \\ \varepsilon_{\theta\theta}^0 \\ \varepsilon_{r\theta}^0 \\ k_{rr} \\ k_{\theta\theta} \\ k_{r\theta} \end{bmatrix}-\begin{bmatrix} N_{rr}^{Tj} \\ N_{\theta\theta}^{Tj} \\ 0 \\ M_{rr}^{Tj} \\ M_{\theta\theta}^{Tj} \\ 0 \end{bmatrix}$$

$$, j=(t,b) \quad (48)$$

The constant coefficients A_{kl}^j, B_{kl}^j and D_{kl}^j (k,l =1, 2, 6) indicate the stretching, bending-stretching, and bending stiffnesses, respectively, which can be obtained by:

$$\begin{aligned}
&\begin{Bmatrix} A_{11}^j \\ B_{11}^j \\ D_{11}^j \end{Bmatrix}=\begin{Bmatrix} A_{22}^j \\ B_{22}^j \\ D_{22}^j \end{Bmatrix}=\int_{-hj/2}^{hj/2}\left(\frac{E_j}{1-\nu_j^{\ 2}}\right)\begin{Bmatrix} 1 \\ z_j \\ z_j^{\ 2} \end{Bmatrix}dz_j \\
&\begin{Bmatrix} A_{12}^j \\ B_{12}^j \\ D_{12}^j \end{Bmatrix}=\int_{-hj/2}^{hj/2}\left(\frac{\nu_j E_j}{1-\nu_j^{\ 2}}\right)\begin{Bmatrix} 1 \\ z_j \\ z_j^{\ 2} \end{Bmatrix}dz_j \\
&\begin{Bmatrix} A_{44}^j \\ B_{44}^j \end{Bmatrix}=\begin{Bmatrix} A_{55}^j \\ B_{55}^j \end{Bmatrix}=\int_{-hj/2}^{hj/2}\left(\frac{E_j}{1+2\nu_j}\right)\begin{Bmatrix} 1 \\ z_j \end{Bmatrix}dz_j \\
&\begin{Bmatrix} A_{66}^j \\ B_{66}^j \\ D_{66}^j \end{Bmatrix}=\int_{-hj/2}^{hj/2}\left(\frac{E_j}{1-\nu_j^{\ 2}}\right)\begin{Bmatrix} 1 \\ z_j \\ z_j^{\ 2} \end{Bmatrix}dz_j
\end{aligned} \quad (49)$$

Also, the thermal stress and moment resultants are defined as:

$$N_{rr}^{Tj}=N_{\theta\theta}^{Tj}=\int_{-hj/2}^{hj/2}\left(\frac{E_j}{1-\nu_j}\alpha_j T_j\right)dz_j \quad (50)$$

$$M_{rr}^{Tj}=M_{\theta\theta}^{Tj}=\int_{-hj/2}^{hj/2}\left(\frac{E_j}{1-\nu_j}\alpha_j T_j\right)z_j dz_j \quad (51)$$

Where E, ν and α are the Young's modulus, the Poisson's ratio and the thermal expansion coefficient, respectively, which in the functionally graded layers are the function of the displacement and the temperature, and in the homogeneous layers are just a function of the temperature. The inertia terms of the face sheets and the core are calculated as follows:

$$\left(I_{0j},I_{1j},I_{2j}\right)=\int_{-hj/2}^{hj/2}\rho_j\left(1,z_j,z_j^{\ 2}\right)dz_j, \qquad \left(j=t,b\right) \quad (52)$$

$$\left(I_{0c},I_{1c},I_{2c},I_{3c},I_{4c},I_{5c},I_{6c}\right)= \int_{-hc/2}^{hc/2}\rho_c\left(1,z_c,z_c^{\ 2},z_c^{\ 3},z_c^{\ 4},z_c^{\ 5},z_c^{\ 6}\right)dz_c \quad (53)$$

The out-of-plane and in plane stresses in the core leads to the high order resultants:

$$Q_{rc},M_{Q1rc},M_{Q2rc}=\int_{-hc/2}^{hc/2}\left(1,z_c,z_c^{\ 2}\right)\sigma_{rz}^c dz_c \quad (54)$$

$$Q_{\theta c},M_{Q1\theta c},M_{Q2\theta c}=\int_{-hc/2}^{hc/2}\left(1,z_c,z_c^{\ 2}\right)\sigma_{\theta z}^c dz_c \quad (55)$$

$$R_{zc},M_{zc}=\int_{-hc/2}^{hc/2}\left(1,z_c\right)\sigma_{zz}^c dz_c \quad (56)$$

$$Q_{r\theta}^c,M_{Q1r\theta}^c,M_{Q2r\theta}^c,M_{Q3r\theta}^c=\int_{-hc/2}^{hc/2}\left(1,z_c,z_c^{\ 2},z_c^{\ 3}\right)\tau_{r\theta}^c dz_c \quad (57)$$

$$R_r^c,M_{r1}^c,M_{r2}^c,M_{r3}^c=\int_{-hc/2}^{hc/2}\left(1,z_c,z_c^{\ 2},z_c^{\ 3}\right)\sigma_{rr}^c dz_c \quad (58)$$

$$R_\theta^c,M_{\theta 1}^c,M_{\theta 2}^c,M_{\theta 3}^c=\int_{-hc/2}^{hc/2}\left(1,z_c,z_c^{\ 2},z_c^{\ 3}\right)\sigma_{\theta\theta}^c dz_c \quad (59)$$

Finally, by substituting the high order stress resultants in the equations of the face sheets and the core in terms of the displacement components, the governing equations of motion are derived in terms of the twenty-three unknowns. However, for a clamped circular sandwich plate, a Galerkin method solution could be established.

3 CLAMPED CIRCULAR SANDWICH PLATE

In order to solve the equations of the free vibration of the clamped FG circular sandwich plate, a Galerkin method with twenty three trigonometric shape functions, which satisfy the boundary conditions, is established. The shape functions can be expressed as:

$$u_{0j} = \left[C_{uj} r sin\lambda r \right] e^{i\omega t} \quad , j = (t, b) \tag{60}$$

$$w_{0j} = \left[C_{wj} \left(cos\lambda r + r\lambda sin\lambda r - \lambda a \right) \right] e^{i\omega t} \tag{61}$$

$$u_k = \left[C_{uk} r sin\lambda r \right] e^{i\omega t} \quad , k = (0,1,2,3) \tag{62}$$

$$w_l = \left[C_{wl} \left(cos\lambda r + r\lambda sin\lambda r - \lambda a \right) \right] e^{i\omega t}; \quad l = (0,1,2) \tag{63}$$

$$\lambda_{rj} = \left[C_{\lambda_{rj}} r sin\lambda r \right] e^{i\omega t} \tag{64}$$

$$\upsilon_{0j} = \upsilon_k = \lambda_{\theta j} = 0 \quad , k = (0,1,2,3) \tag{65}$$

$$\lambda_{zj} = \left[C_{\lambda_{zj}} \left(cos\lambda r + r\lambda sin\lambda r - \lambda a \right) \right] e^{i\omega t} \tag{66}$$

where "C_{uj}, C_{wj}, C_{uk}, C_{wl}, $C_{\lambda rj}$ and $C_{\lambda zj}$" are fifteen unknown constants and $\lambda=\pi/2a((2n-1))$ that "n" is the wave number. Since the plate is axisymmetric, "Eqs. (26, 29, 35, 36, 37, 38, 43, and 46)" are eliminated and the number of the equations is reduced to fifteen. On the other hand, these fifteen equations are not independent and by a procedure, the number of them is reduced. Lagrange constants can be isolated as the faces constants.

It is seen that based on the compatibility conditions, the unknown constants of the faces are dependent to the core constants. At last by some operations the number of the equations are reduced to seven in terms of the core unknown constants. The seven equations can be written in the 7×7 matrix form which include the mass, "M", and stiffness, "K", matrices in accordant to the "Eq. (67)" to obtain the constant Eigen values which equals to Eigen frequencies, ω_n, for every wave number, n:

$$(k_n - \omega_n^2 M_n) F_n = 0 \tag{67}$$

In "Eq. (67)", F_n is the Eigen vector which determines the seven unknown constants of the core. To simplify, the fundamental frequency parameter defined that is non-dimensional as:

$$\bar{\omega} = \frac{\omega a^2}{h} \sqrt{\frac{\rho_0}{E_0}} \tag{68}$$

where "a" is the radius of circular sandwich plate; "h" is the total thickness of sandwich plate; ρ_0 is density equal to 1kg/m^3 and E_0 is the young module equal to 1 GPa.

4 VERIFICATION AND NUMERICAL RESULTS

To validate the approach of this work, the present results in a special case are compared with results of [14], [36] and FEM results of Abaqus software for a clamped isotropic circular plate with properties: E=380 (GPa), ρ=3800 (Kg/m^3), ϑ =0.3 and h/a=0.2 as shown in "Table 1". Because, the theory of present analysis is different from the [14], [36], a discrepancy is found in the results. Also, discontinues model is used in Abaqus model that causes a little discrepancy with present analysis.

Table 1 Comparison of fundamental frequency parameters of present, [13], [36] and Abaqus results

M	Present result	[14]	[36]	ABAQUS
1	10.232	10.213	10.216	10.842
2	21.472	21.259	21.260	22.318

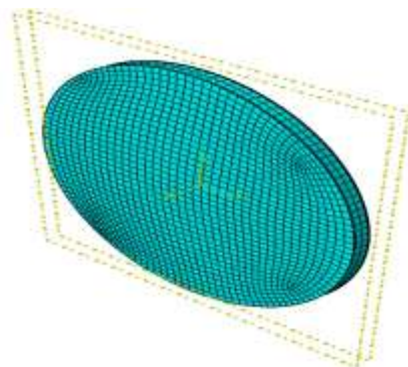

Fig. 2 Finite element model for the clamped sandwich plate.

Now, another numerical problem will be discussed to more investigation of the present approach. Consider two kinds of clamped FG circular sandwich plates. In type-I, the face sheets interior planes and the core are made of the zirconium dioxide and the outer planes of the faces are made of silicon nitride. In type-II, the interior plane of the core and inner face sheet are made of the zirconium dioxide and the outer plane of the core and outer face sheet are made of silicon nitride. The properties of these materials are available in [32].

Variation of the material properties in each FG layer is correspond to the modified power-law function. Numerical examples are simulated by Abaqus software for validation of the present approach as shown in “Fig. 2”.

In “Table 2” fundamental frequency parameters of this approach are compared with the FEM results by Abaqus software in the temperature of the room and for different power law indices in the case of 1-8-1 sandwich. It should be noted that in 1-8-1 sandwich, the core thickness is eight times of every face sheets thickness and the structure is symmetric. In “Table 2”, the discrepancies between the present results and FEM results are due to simulation method of FG layers in Abaqus software. In order to simulate the FG face-sheets and FG core in Abaqus, all FG layers are divided to 20 isotropic sub-layers that each sublayer has different properties according to power law function. There is a good agreement between the present study results and the FEM results obtained by Abaqus.

Table 2 Comparison of fundamental frequency parameters of the present method and Abaqus results in 1-8-1 sandwich

	N	Present method	Abaqus	Discrepancy
Type-I	0.2	0.76734	0.72906	%5.25
	1	0.75616	0.7237	%4.48
	2	0.74972	0.7131	%5.13
Type-II	0.2	1.0726	1.0501	%2.14
	1	0.9425	0.9385	%4.26
	2	0.8786	0.8551	%2.74

The frequency of the structures is dependent to the temperature variation. The effect of the uniform temperature distribution on the fundamental frequency parameter is depicted in “Fig. 3” for two types of 1-8-1 clamped circular FG sandwich plates in different power law indices. As shown in “Fig. 3”, while the temperature is increased, the fundamental frequency parameter decreases. According to “Eq. (6)”, temperature rising reduces the strength of the material. To clarify this phenomena, in Table 3 the effect of temperature on the Young's modulus of ceramic and metal is indicated. With increasing the temperature, modulus of metal and ceramic decrease, but due to the microstructural reasons, decreasing the module of metal is more. So, increasing the temperature reduces the mechanical properties that is one of the most important reason in decreasing the frequency in high temperature. Also in a constant temperature, the fundamental frequency is decreased in the larger power law indices; since with increasing the power-law index the properties of the layers are tending to metal and the strength of the structure is decreased. It is obvious in “Fig. 3” that the values of the fundamental frequency parameters in type- II are more than type-I for all power law indices and all temperatures. It is concluded that the sandwiches with FG core is proper than the sandwiches with FG face sheets, in the thermal conditions, generally.

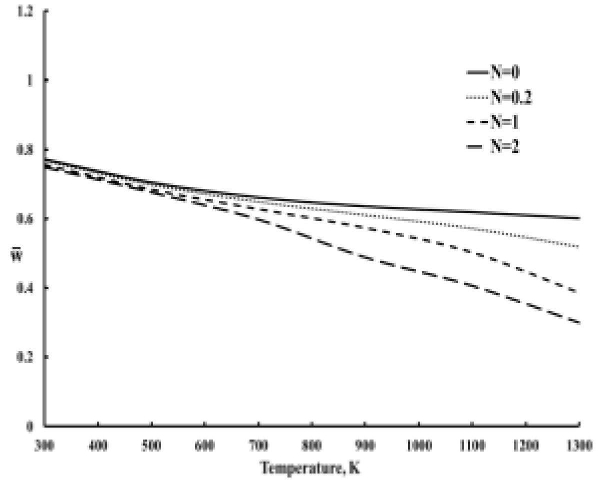

(a): Sandwich type-I

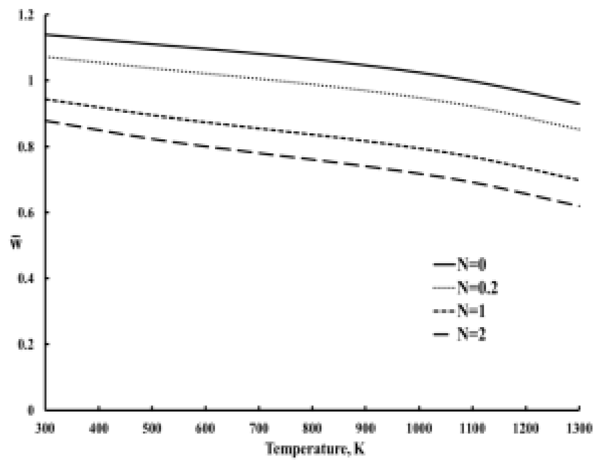

(b): Sandwich type-II

Fig. 3 Frequencies changing with temperature in various power law indices for 1-8-1 sandwich plates.

Table 3 Effect of temperature variation on the Young modulus in metal and ceramics

Temperature	Silicon Nitride	Zirconium dioxide
300 K	322.27 (GPa)	168.06 (GPa)
1300 K	268.08 (Gpa)	112.52 (GPa)
change	16.81%	33.04%

Figure 4 shows the radius to thickness ratio changing on the fundamental frequency parameter for 1-8-1 circular FG sandwich plates in temperature of the room. This figure implies that when ratios increase for constant power law index, the fundamental frequency parameters increase. As depicted in “Fig. 4”, power law effects on the FG core sandwiches are more than FG faces sandwiches.

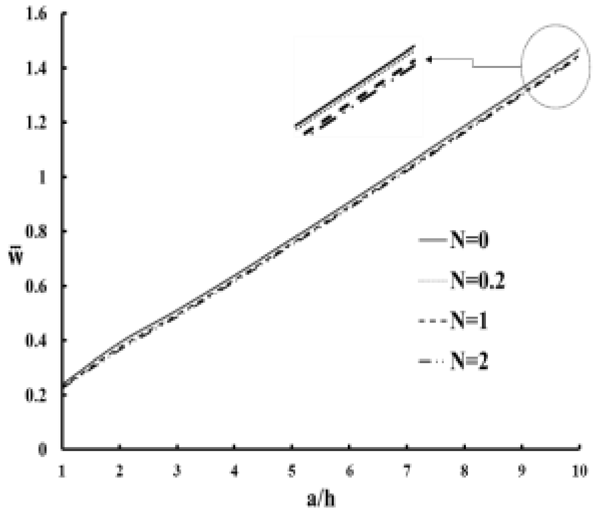

(a): Sandwich type-I

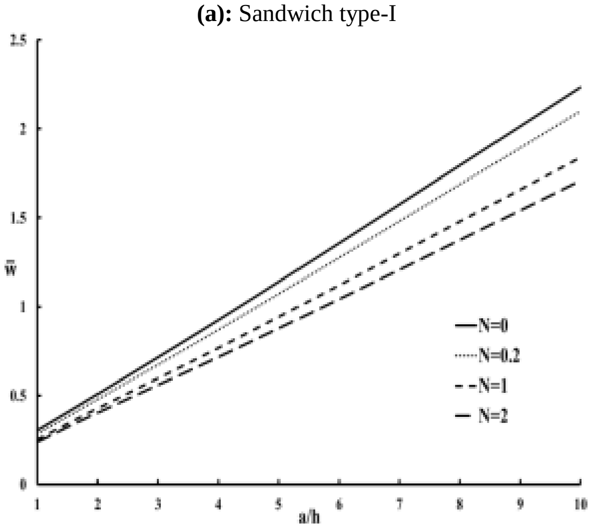

(b): Sandwich type-II

Fig. 4 Variation of the fundamental frequency with radius to thickness ratio for different power law indices in 1-8-1 sandwiches.

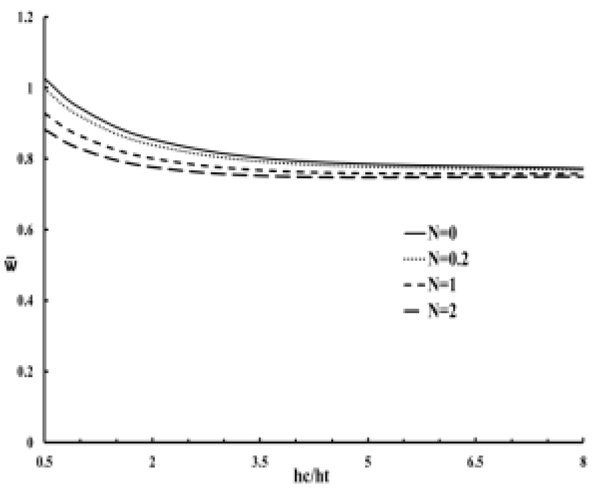

(a): Sandwich type-I

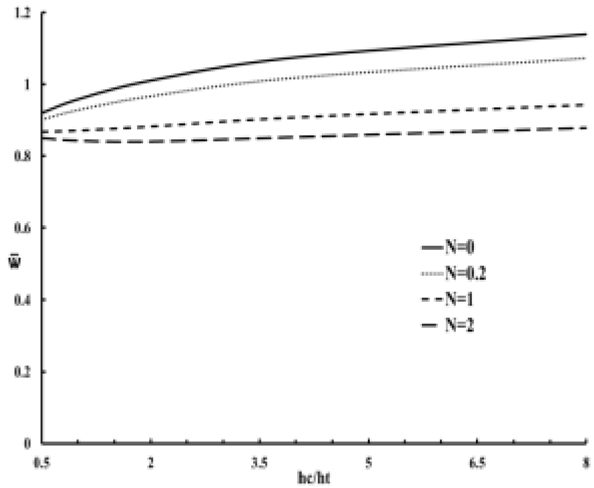

(b): Sandwich type-II

Fig. 5 Fundamental frequency changing with core to face sheet thickness ratio in various power law indices.

Figure 5 depicts variation of the core to face sheet thickness ratio, h_c/h_t, on the fundamental frequency parameter in various power law indices and constant total thickness. In type-II, by increasing the ratio, the amount of ceramic is increased and the structure will be stiffer, so, the fundamental frequency parameter increases. But, in type-I, by increasing the ratio in a constant total thickness, the amount of metal increases and the structure will be softer, so the fundamental frequency decreases.

In order to clearly understand the porosity influence, “Figs. 6 and 7” show the effect of even and uneven porosity distributions on the frequency of the sandwich plates, respectively. As depicted in these figures, in sandwiches type-II, both porosity distributions are dependent of power law indices. By increasing the porosity volume fraction, the fundamental frequency parameter first increases at lower gradient indices, but from a certain value of the power law index, increasing porosity volume leads to decreasing the fundamental frequency parameter.

These increasing and decreasing are stronger in the case of even porosity distribution in FG faces sandwiches. In even distributions, porosities occur all over the cross-section of FG layer. While, in uneven distribution, porosities are available at middle zone of cross section. Beside, in “Figs. 6 and 7” in sandwiches type-I, with increasing the porosity volume fraction, the fundamental frequency parameters increase with an almost constant slope for all power law indices that shows another important different behaviour of these two kinds of sandwiches.

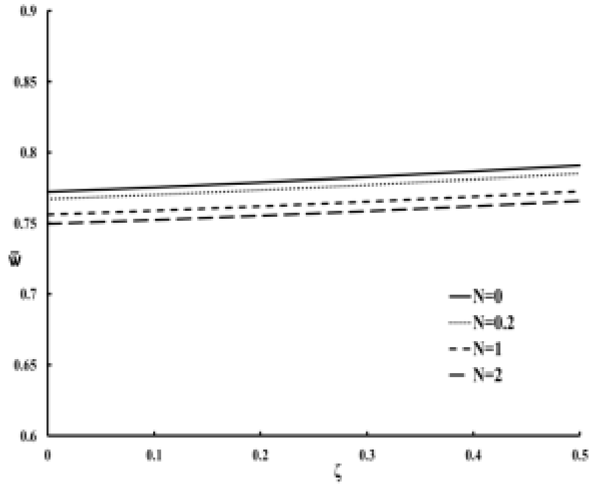

(a): Sandwich type-I

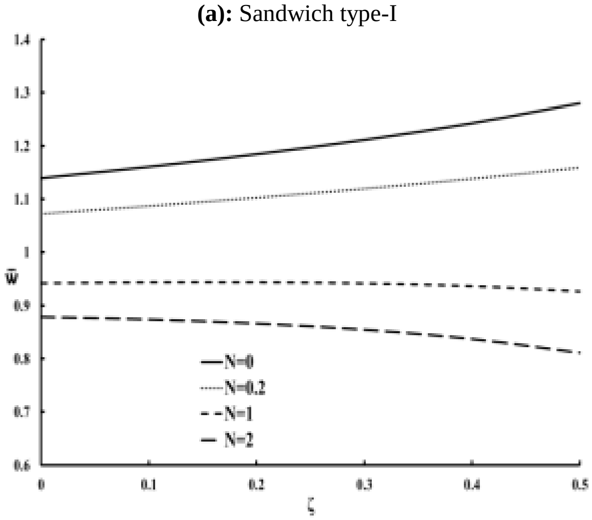

(b): Sandwich type-II

Fig. 6 Variation of the fundamental frequency with even porosity distribution for different power law indices.

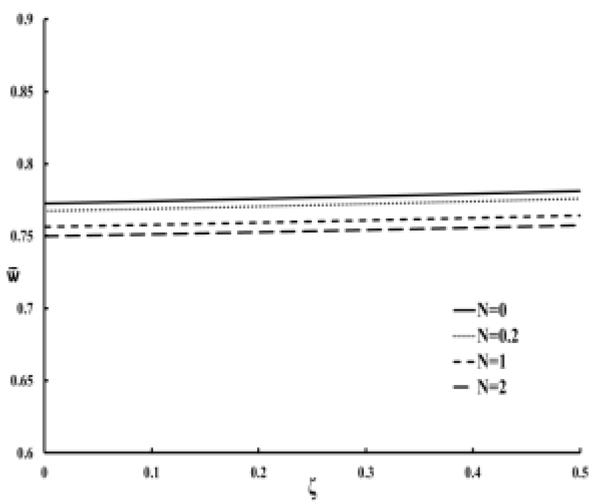

(a): Sandwich type-I

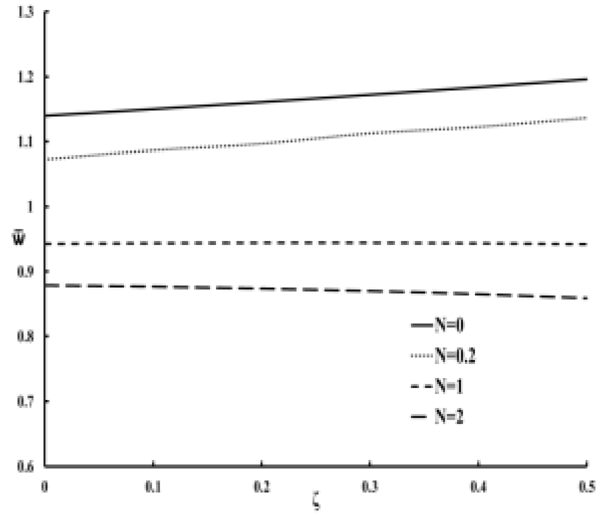

(b): Sandwich type-II

Fig. 7 Variation of the fundamental frequency with uneven porosity distribution for different power law indices.

5 CONCLUSION

In this paper by applying a modified high order theory, vibration behaviour of two types of clamped circular sandwich plates were investigated subjected to a uniform high temperature distribution. Governing equations were derived based on the Hamilton's energy principle. Material properties of the FG layers were temperature and location dependent. By considering two types of porosity in FG layers, a modified power law rules was employed to model the gradually variation of the properties. The homogeneous layers were temperature dependent, too. Unlike the most papers, in plane and out of plane stresses of the core were considered at the same time. To obtain the frequencies, a Galerkin method was applied. In order to validate present approach, the numerical results which were obtained by Abaqus software were compared to the results of this analytical approach and for a special case compared with some literature. Based on the results obtained by this approach and comparing with FEM results, there was a good agreement with them and the following conclusion can be drawn.

1- With increasing the temperature in a constant power law index, the fundamental frequency parameter decreases.

2- By increasing the power law index, the fundamental frequency parameter decreases.

3- With increasing the radius to thickness ratio, the fundamental frequency parameter increases.

4- By increasing the core to face sheet thickness ratio, the fundamental frequency parameter in type-II increases and in type-I it decreases.

5- In sandwiches type-II, both porosity distributions are dependent of power law indices, but in type-I with increasing the porosity volume fraction in both even and uneven distributions, the fundamental frequency parameter increases.

6- Generally, Power law effects on the FG core sandwiches are more than FG faces sandwiches.

6 NOMENCLATURE

δ	Variation	B	Bending-stretching stiffnesses
K	Kinetic Energy (J)	D	Bending stiffnesses
U	Strain Energy (J)	k	
t	Time (s)	E	Young's modulus
ρ	Density(kg/m^3)	ν	Poisson's ratio
u	Inplane deformation	α	thermal expansion coefficient
υ	Inplane deformation	ω	Frequency
w	Transverse deformation	N	Power law index
r, θ, z	Polar coordinate components	n	Wave number
T	Temperature(K)	N	Stress Resultant
ζ	Porosity volume fraction	M	Moment Resultant
c e	Ceramic	$()_{,i}$	Derivation
m	Metal	A	Stretching stiffnesses
σ	Normal stresses		
ε	Normal strain		
τ	Shear stress		
γ	Shear stress		
λ	Lagrange multiplier		
I	Inertial Terms		

REFERENCES

[1] Fazzolari, F. A., Sandwich Structures. In Stability and Vibrations of Thin Walled Composite Structures, Woodhead Publishing, 2017, pp. 49-90.

[2] Mahamood, R. M., Akinlabi, E. T., Functionally Graded Materials, Springer, Gewerbestrasse, Switzerland, 2017, pp. 1-118.

[3] Boutahar, L., Benamar, R., A Homogenization Procedure for Geometrically Non-linear Free Vibration Analysis of Functionally Graded Annular Plates with Porosities, Resting on Elastic Foundations, Ain Shams Engineering Journal, Vol. 7, No. 1, 2016, pp. 313-333.

[4] Reddy, J. N., Analysis of Functionally Graded Plates. International Journal for Numerical Methods in Engineering. Vol. 47, No. 1- 3, 2000, pp. 663-684.

[5] Frostig, Y., Baruch, M., Vilnay, O., and Sheinman, I., High-Order Theory for Sandwich-Beam Behavior with Transversely Flexible Core, Journal of Engineering Mechanics, Vol. 118, No. 5, 1992, pp. 1026-1043.

[6] Najafizadeh, M. M., Shoughi, P., Three Dimensional Free Vibration of FGM Circular Plates Using Semi-Analytical Method, Advance Design and Manufacturing Technology, Vol. 3, No. 1, 2009, pp. 41-49.

[7] Zenkour, A. M., Sobhy, M., Thermal Buckling of Various Types of FGM Sandwich Plates, Composite Structures, Vol. 93, No.1, 2010, pp. 93-102.

[8] Amininejad, R., Mohajerani, A. R., Samsami A. R., and Amininejad, S., Free Vibration Analysis of S-FGM-Coated and S-FGM-Undercoated Plates with Classical Boundary Conditions, Advance Design and Manufacturing Technology, Vol. 3, No. 1, 2009, pp. 19-30.

[9] Davar, A., Khalili, S. M. R., and Hadavinia, H., Free Vibrations of Functionally Graded Circular Cylindrical Shells under Internal Pressure, Advance Design and Manufacturing Technology, Vol. 6, No. 4, 2013, pp. 49-58.

[10] Kamarian, S., Volume Fraction Optimization of Four-Parameter FGM Beams Resting on Elastic Foundation, Advance Design and Manufacturing Technology, Vol. 6, No. 4, 2013, pp. 75-82.

[11] Wang, Y. Q., Jean W. Z., Vibration Behaviors of Functionally Graded Rectangular Plates with Porosities and Moving in Thermal Environment, Aerospace Science and Technology, Vol. 69, 2017, pp. 550-562.

[12] Barati, M. R, Shahverdi, H., Aero-Hygro-Thermal Stability Analysis of Higher-order Refined Supersonic FGM Panels with Even and Uneven Porosity Distributions, Journal of Fluids and Structures, Vol. 73, 2017, pp. 125-136.

[13] Chen, D., Yang, J., and Kitipornchai, S., Elastic Buckling and Static Bending of Shear Deformable Functionally Graded Porous Beam, Composite Structures, Vol. 133, 2015, pp. 54-61.

[14] Prakash, T., Ganapathi, M., Asymmetric Flexural Vibration and Thermo Elastic Stability of FGM Circular Plates using Finite Element Method, Composites Part B: Engineering, Vol. 37, 2006, pp. 642–649.

[15] Heydari, A., Analytical Solutions for Buckling of Functionally Graded Circular Plates under Uniform Radial Compression by using Bessel Function, Advance Design and Manufacturing Technology, Vol. 6, No. 4, 2013, pp. 41-47.

[16] Jandaghian, A., Jafari, A., Investigating Effect of Using Piezoelectric layers on the Forced Vibration of Circular Plates, Advance Design and Manufacturing Technology, Vol. 5, No. 5, 2012, pp. 1-9.

[17] Morovat, F., Analytical Solution for Buckling of Composite Sandwich Truncated Conical Shells subject to Combined External Pressure and Axial Compression Load, Advance Design and manufacturing Technology, Vol. 8, No. 4, 2015, pp. 83-94.

[18] Mantari J. L., Granados E. V., and Guedes S. C., Vibrational Analysis of Advanced Composite Plates Resting on Elastic Foundation, Composites Part B: Engineering, Vol. 66, 2014, pp. 407–19.

[19] Khalili, S. M. R., Mohammadi, Y., Free Vibration Analysis of Sandwich Plates with Functionally Graded Face Sheets and Temperature-Dependent Material Properties: A New Approach, European Journal of Mechanics - A/Solids, Vol. 35, 2012, pp. 61-74.

[20] Salami, S. J., Dariushi, S., Sadighi, M., and Shakeri, M., An Advanced High-order Theory for Bending Analysis of Moderately Thick Faced Sandwich Beams, European Journal of Mechanics - A/Solids, Vol. 56, 2016, pp. 1–11.

[21] Frostig, Y., Birman, V., and Kardomateas, G. A., Non-Linear Wrinkling of a Sandwich Panel with Functionally Graded Core–Extended High-order Approach, International Journal of Solids and Structures, Vol. 148, 2018, pp. 122-139.

[22] Shahrjerdi, A., Mustapha, F., Bayat, M., and Majid, D. L. A., Free Vibration Analysis of Solar Functionally Graded Plates with Temperature-Dependent Material Properties using Second Order Shear Deformation Theory, Journal of Mechanical Science and Technology, Vol. 25, No. 9, 2011, p. 2195.

[23] Frostig, Y., Thomsen, O. T., On the Free Vibration of Sandwich Panels with a Transversely Flexible and Temperature Dependent Core Material-Part II: Numerical Study, Composites Science and Technology, Vol. 69, 2009, pp. 863–869.

[24] Pandey, S., Pradyumna, S., Free Vibration of Functionally Graded Sandwich Plates in Thermal Environment using a Layer-Wise Theory, European Journal of Mechanics - A/Solids, Vol. 51, 2015, pp. 55–66.

[25] Sherif, H. A., Free Flexural Vibrations of Clamped Circular Sandwich Plates, Journal of Sound and Vibration, Vol. 157, No. 3, 1992, pp. 531-537.

[26] Chan, P., Frequency Equation for the In-plane Vibration of a Clamped Circular Plate, Journal of Sound and Vibration, Vol. 313, 2008, pp. 325–333.

[27] Nie, G. J., Zhong, Z., Semi-Analytical Solution for Three-Dimensional Vibration of Functionally Graded Circular Plates. Computer Methods in Applied Mechanics and Engineering, Vol. 196, No. 49-52, 2007, pp. 4901-4910.

[28] Ebrahimi, F., Rastgoo, A., and Kargarnovin, M. H., Analytical Investigation on Axisymmetric Free Vibrations of Moderately Thick Circular Functionally Graded Plate Integrated with Piezoelectric Layers, Journal of mechanical science and technology, Vol. 22, No. 6, 2008, pp. 1058-1072.

[29] Lal, R., Rani, R., On Radially Symmetric Vibrations of Circular Sandwich Plates of Non-Uniform Thickness, International Journal of Mechanical Sciences, Vol. 99, 2015, pp. 29-39.

[30] Heshmati, M., Jalali, S. K., Effect of Radially Graded Porosity on the Free Vibration Behavior of Circular and Annular Sandwich Plates, European Journal of Mechanics-A/Solids, Vol. 74, 2019, pp. 417-430.

[31] Reddy, J. N., Mechanics of Laminated Composite Plates and Shells, Theory and Application, CRC Press, New York, USA, 2003.

[32] Shen, H. S., Functionally Graded Materials Nonlinear Analysis of Plates and Shells, CRC Press, New York, 2009.

[33] Kiani, Y., Eslami, M.R., Instability of Heated Circular FGM Plates on a Partial Winkler-type Foundation, Acta Mechanica, Vol. 224, No. 5, 2013, pp. 1045-1060.

[34] Kim, Y. W., Temperature Dependent Vibration Analysis of Functionally Graded Rectangular Plates, Journal of Sound and Vibration, Vol. 284, No. 3-5, 2005, pp. 531-549.

[35] Es'haghi, M., Hashemi, S. H., and Fadaee, M., Vibration Analysis of Piezoelectric FGM Sensors using an Accurate Method, International Journal of Mechanical Sciences, Vol. 53, No. 8, 2011, pp. 585-594.

[36] Wu, T. Y., Wang, Y. Y., Liu, and G. R., Free Vibration Analysis of Circular Plates using Generalized Differential Quadrature Rule, Computer Methods in Applied Mechanics and Engineering, Vol. 191, No. 46, 2002, pp. 5365-5380.